CHEMISTRY OF MATERIALS
Cite This: Chem. Mater. 2018, 30, 2945−2953
Article
pubs.acs.org/cm

The Role of the Side Chain on the Performance of N-type Conjugated Polymers in Aqueous Electrolytes

Alexander Giovannitti,[*,†,‡] Iuliana P. Maria,[†] David Hanifi,[§] Mary J. Donahue,[∥] Daniel Bryant,[⊥] Katrina J. Barth,[#] Beatrice E. Makdah,[#] Achilleas Savva,[□] Davide Moia,[‡] Matyáš Zetek,[‡] Piers R.F. Barnes,[‡] Obadiah G. Reid,[▽,■] Sahika Inal,[□] Garry Rumbles,[△,▽,■] George G. Malliaras,[●] Jenny Nelson,[‡] Jonathan Rivnay,[*,#,○] and Iain McCulloch[†,⊥]

[†]Department of Chemistry, Imperial College London, London SW7 2AZ, United Kingdom
[‡]Department of Physics and Centre for Plastic Electronics, Imperial College London, London SW7 2AZ, United Kingdom
[§]Department of Chemistry, Stanford University, Stanford, California 94305, United States
[∥]Department of Bioelectronics, École Nationale Supérieure des Mines, CMP-EMSE, MOC Gardanne 13541, France
[⊥]Physical Sciences and Engineering Division, KAUST Solar Center (KSC), King Abdullah University of Science and Technology (KAUST), KSC Thuwal 23955-6900, Saudi Arabia
[#]Department of Biomedical Engineering, Northwestern University, 2145 Sheridan Road, Evanston, Illinois 60208, United States
[□]Biological and Environmental Science and Engineering, King Abdullah University of Science and Technology (KAUST), Thuwal 23955-6900, Saudi Arabia
[○]Simpson Querrey Institute for BioNanotechnology, Northwestern University, Chicago, Illinois 60611, United States
[△]Department of Chemistry and Biochemistry, University of Colorado at Boulder, Boulder, Colorado 80309, United States
[▽]Renewable and Sustainable Energy Institute, University of Colorado at Boulder, Boulder, Colorado 80309, United States
[■]Chemistry and Nanoscience Center, National Renewable Energy Laboratory, 15013 Denver West Parkway, Golden, Colorado 80401, United States
[●]Electrical Engineering Division, University of Cambridge, 9 JJ Thomson Avenue, Cambridge CB3 0FA, United Kingdom

Supporting Information

ABSTRACT: We report a design strategy that allows the preparation of solution processable n-type materials from low boiling point solvents for organic electrochemical transistors (OECTs). The polymer backbone is based on NDI-T2 copolymers where a branched alkyl side chain is gradually exchanged for a linear ethylene glycol-based side chain. A series of random copolymers was prepared with glycol side chain percentages of 0, 10, 25, 50, 75, 90, and 100 with respect to the alkyl side chains. These were characterized to study the influence of the polar side chains on interaction with aqueous electrolytes, their electrochemical redox reactions, and performance in OECTs when operated in aqueous electrolytes. We observed that glycol side chain percentages of >50% are required to achieve volumetric charging, while lower glycol chain percentages show a mixed operation with high required voltages to allow for bulk charging of the organic semiconductor. A strong dependence of the electron mobility on the fraction of glycol chains was found for copolymers based on NDI-T2, with a significant drop as alkyl side chains are replaced by glycol side chains.

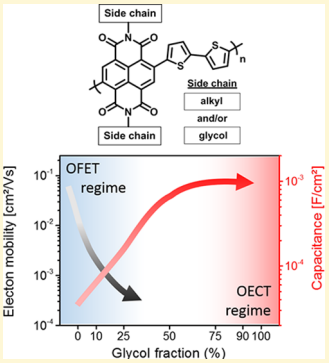

INTRODUCTION

Over the past few years, conjugated polymers containing ethylene glycol (from here onward, "glycol") side chains have received increasing attention in the field of organic electronics. Polymers have been specially designed to improve performance of organic photovoltaics (OPV),[1,2] organic field effect transistors (OFET),[1,3,4] and organic electrochemical transistors (OECT).[5−8] Glycol side chains have been reported to facilitate ion transport in conjugated polymers, allowing ions to penetrate into the bulk during electrochemical redox reactions in aqueous electrolytes. This is an important characteristic of so-called "mixed conductors", which require optimal transport of both electronic charge carriers (holes and electrons) and ions (cations and anions).[6,9,10] When comparing alkyl side chains to glycol side chains, intra- and intermolecular interaction forces stem from different origins. The dominant interactions of alkyl side chains can be described as dispersion forces,[11] while the substitution of methylene groups (CH_2) for oxygen atoms introduce permanent dipoles within the

Received: January 23, 2018
Revised: April 12, 2018
Published: April 24, 2018

DOI: 10.1021/acs.chemmater.8b00321
Chem. Mater. 2018, 30, 2945−2953

side chains, strongly affecting the intra- and interchain interactions of the side chain. The substitution of alkyl by glycol chains on the same backbone can increase the dielectric constant[1] and decrease the $\pi-\pi$ stacking distance of the backbone,[1,2,6] enabling enhanced swelling in aqueous solutions[6,12,13] and chelation of cations.[14,15] In addition, polar side chains have been shown to improve the doping efficiency of copolymers in thermoelectric devices, mostly because of a higher miscibility of the dopant within the polar side chain.[16−19]

The magnitude of signal amplification of OECTs is reflected in the performance of the material through the transconductance $g_m = \partial I_d/\partial V_g$, which may be seen as the figure of merit.[20] To meaningfully compare and benchmark the performances of novel materials for OECTs, devices with comparable physical dimensions and biasing may be fabricated and tested. Mixed conductors have been successfully employed as the active layer in both accumulation[5,6,21] and depletion mode OECTs,[20,22−24] where high transconductance values in the mS range were reported,[5,6,24] which is mostly attributed to the ability of the active layer to achieve volumetric charging. Because OECTs are usually operated in aqueous electrolytes, low turn-on and operation voltages are required to avoid undesirable electrochemical reactions such as water-splitting or oxygen reduction.[25] A combination of both high transconductance and low operational voltage makes the device highly interesting for the detection of biological events.[26,27] Depletion mode OECTs based on the conducting polymer blend poly(3,4-ethylenedioxythiophene)-poly(styrenesulfonate) (PEDOT:PSS) have successfully been used for recordings of brain activity[22,28] as well as the heart beat (ECG recordings).[23] However, depletion mode devices bear a number of drawbacks. Notably, they are "on" in the resting, zero gate bias state, meaning that they draw significant current, raising concerns for power consumption. In recent years, novel redox-active copolymers have been developed for p-type accumulation mode OECTs, showing high transconductance and stability as well as the advantage of depositing the active layer from low boiling solvent without further cross-linking or annealing steps.[5,6] The latter is important for large scale production of printed biosensors where device-to-device reproducibility is critical.[29,30] Recently, we reported the development of an accumulation mode ambipolar OECT based on naphthalene-1,4,5,8-tetracarboxylic-diimide-alkoxybithiophene p(gNDI-gT2), a copolymer with a low reduction and oxidation potential (vs Ag/AgCl), enabling stable operation of p- and n-type OECTs in aqueous electrolytes.[7] To date, the performance of the n-type OECT is low compared to state of the art p-type OECT materials.

Here, we report on the development of donor−acceptor copolymers based on naphthalene-1,4,5,8-tetracarboxylic-diimide-bithiophene (NDI-T2) and study how the properties are affected when a fraction of the alkyl side chains is substituted by glycol side chains. Additionally, the influence of introduced glycol chains on the electron mobility is investigated, taking the high electron mobility alkylated copolymer P(NDI2OD-T2) as a reference.[31] Because several biological processes involve the transfer of electrons (e.g., enzymatic reactions), the development of materials which can accept electrons and stabilize them in aqueous solutions represents an interesting approach for the development of novel sensor technologies, e.g. the detection of biomolecules in biological media.

EXPERIMENTAL SECTION

Synthesis of the Copolymers. The synthesis of the copolymers is reported in the Supporting Information (Section 2).

Electrochemical Measurements. Cyclic voltammograms were recorded using a potentiostat (Ivium Compactstat) with a standard three-electrode setup with ITO coated glass substrates as the working electrode, a platinum mesh as the counter electrode, and a Ag/AgCl reference electrode. The measurements were carried in degassed 0.1 M NaCl aqueous solution at a scan rate of 100 mV/s. Electrochemical impedance spectroscopy was performed with a three electrode configuration using a potentiostat (Metrohm Autolab) with platinum and Ag/AgCl counter and reference electrodes, respectively. The polymer coated gold electrode was the working electrode, and the electrolyte was a 0.1 M NaCl aqueous solution. Effective capacitance was determined from $C \sim 1/(2\pi f Im(Z))$, where f is the frequency and Z is the complex impedance; this capacitance was confirmed for doped spectra from a fit to a $R(R\|C)$ equivalent circuit to extract both capacitance per unit area and C^*. Analysis was performed with Metrohm NOVA software and custom MATLAB tools.

Transistor Fabrication and Characterization. Organic field effect transistors (OFETs) were fabricated with a bottom-contact top-gate architecture. A 40 nm Ag source and drain electrodes with a length of 40 μm and a width of 1000 μm were evaporated onto precleaned borofloat glass (Semiconductor Wafer Inc.) through a shadow mask. Active layer polymer films were deposited by spin coating from a 10 mg/mL chloroform solution while the solution was at 60 °C. After deposition, the films were annealed for 5 min at 70 °C and left for 12 h in a sealed chamber with desiccant to remove any residual moisture. Subsequently, a CYTOP dielectric layer was deposited on the surface of the active layer by spin coating at 2100 rpm to obtain a layer with 900 nm thickness. A thin layer of aluminum (60 nm) was evaporated through a shadow mask to obtain a gate electrode. All measurements were performed inside a glovebox at room temperature using a Keysight B2912A Sourcemeter and probe station set up.

OECTs were fabricated as previously reported;[22,32] the conjugated polymers were deposited by spin coating (thin films) or drop casting (thick films) from chloroform (5 mg/mL) before sacrificial peel off of Parylene C for the dry patterning processes. The completed samples were not annealed or treated after deposition; the samples were briefly rinsed in deionized water before testing. OECT IV curves (transfer and output) as well as repetitive pulsing were performed with a Keithley 2400 source-measure unit and custom LabView scripts. Analysis was performed with MATLAB.

Time-Resolved Microwave Conductivity (TRMC). TRMC experiments were conducted in a setup that has been previously described in thorough detail.[33] Briefly, the change in microwave (~9 GHz) power absorbed by a sample was measured in response to a short (4−5 ns fwhm) laser pulse. The fractional microwave power absorption is converted to a photoconductance through numerical calculation of the sensitivity of the apparatus, given by K (23 000 S^{1-} in this case). In the experiments reported here, all samples were excited with 700 nm light at a fluence between 2×10^{14} and 2×10^{15} photons/cm^2. Samples were sealed inside the cavity and purged with nitrogen for the duration of all microwave measurements. Photoluminescence spectra were measured in the same setup as the microwave conductivity experiments, in air, using 600 nm pulsed laser excitation and a 650 nm long-pass filter. Luminescence is collected from the microwave sample cavity using a 50 mm f/0.95 camera lens. A fiber patch cable is mounted at the focal plane of the lens and coupled to a Princeton Instruments SpectraPro 2500i spectrometer equipped with a silicon CCD camera. The intensity-correction curve for this complete optical detection apparatus was obtained by measuring the spectrum of a standard tungsten−halogen lamp (Ocean Optics DH-2000). Thin-film samples for TRMC and photoluminescence (PL) experiments were prepared by drop-casting 100 μL of polymer solution (10 mg/mL, chloroform) onto fused quartz substrates in a nitrogen glovebox at room temperature.

RESULTS AND DISCUSSION

The synthesis of the 2,6-dibromonaphthalene-1,4,5,8-tetracarboxylic-diimide (NDI) monomer with a linear glycol chain (g7-NDI-Br$_2$) is presented in Figure 1a. The methyl end-capped heptakis(ethylene glycol) chain with an amine end group was

DOI: 10.1021/acs.chemmater.8b00321
Chem. Mater. 2018, 30, 2945−2953

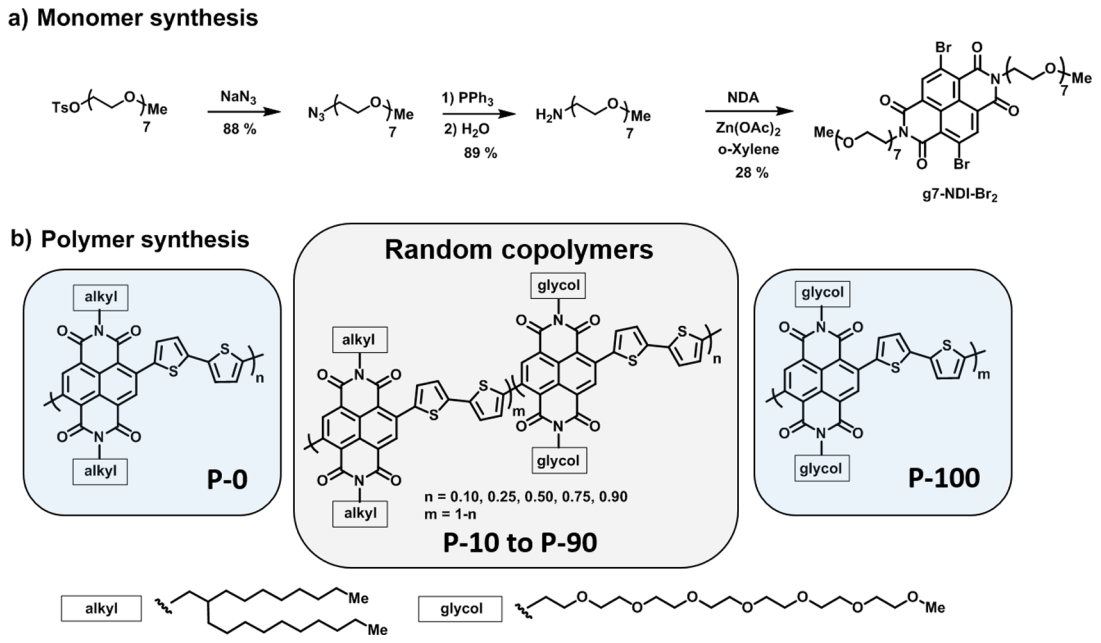

Figure 1. Synthesis of the monomer g7-NDI-Br_2 and NDI-T2 copolymers P-0, P-10, P-25, P-50, P-75, P-90, and P-100 representing 0, 10, 25, 50, 75, 90, and 100% glycol chain percentages.

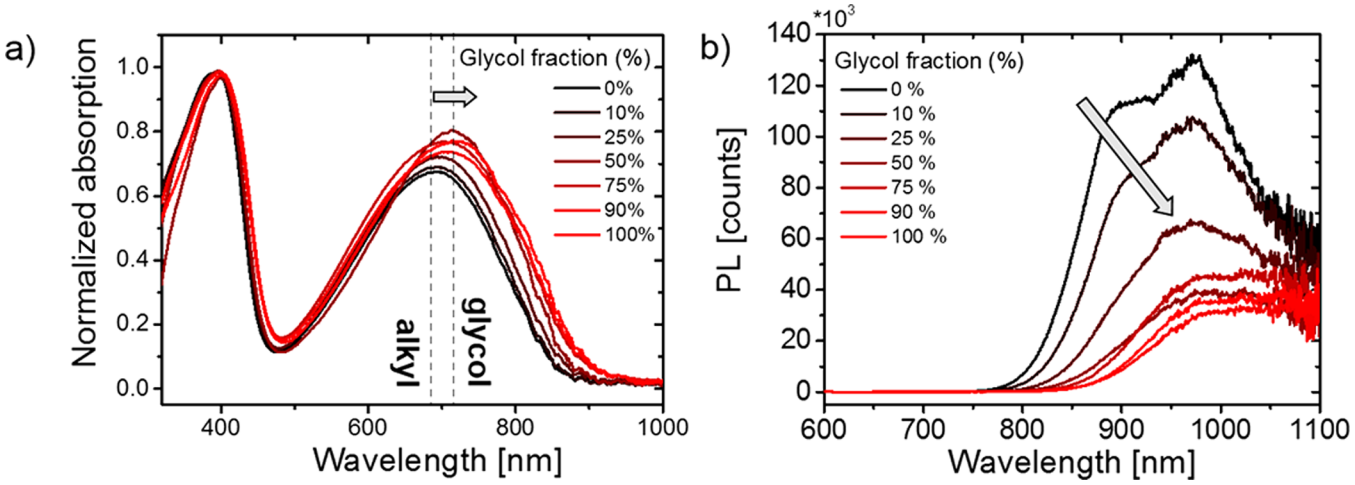

Figure 2. (a) Thin film UV−vis absorption spectra of the copolymers on glass substrates, spun cast from chloroform and (b) PL spectra of the polymer series in solid state excited with a laser pulse at 600 nm (see Supporting Information Figure S22, for the correction procedure of the for the PL data).

prepared starting from tetraethylene glycol and triethylene glycol monomethyl ether according to literature procedures.[33,34] For the final step of the monomer synthesis (diimide formation), a new procedure was developed to suppress the nucleophilic aromatic substitution (S_NAr) reaction of the amine and the NDI core, a side reaction which forms secondary amines and occurs especially in polar solvents.[35] To suppress the formation of this side-product, *o*-xylene was used as the reaction solvent in combination with zinc acetate, acting as a weak Lewis acid to catalyze the ring closure to form the diimides. The effect of the choice of the solvent on the product formation is shown in Figure S14, where it can be observed that using polar solvents such as DMF or carboxylic acids[4] significantly increase the formation of diamines. Because the glycol side chains increase the solubility of the polymers in polar chlorinated solvents, a branching point is not necessary for glycol side chains. The 2-octyldodecyl alkyl chain monomer NDI2OD-Br_2 was prepared according to the literature.[36] Finally, random copolymers were prepared by Stille polymerization in chlorobenzene at 130 °C (Figure 1b); synthetic protocols are described in the Supporting Information.

The copolymers are soluble in chloroform and chlorobenzene, while copolymers containing >75% glycol chain polymers tend to aggregate in chlorobenzene and dissolve only when heated above 80 °C. The solution UV−vis absorbance spectra of the polymers in chlorobenzene are presented in Figure S16a, where an increased aggregation was observed for copolymers with higher glycol percentages. The opposite trend is observed in chloroform where copolymers with larger glycol percentages have a higher solubility and show less aggregation (Figure S16b). The UV−vis absorption spectra in the solid state are shown in Figure 2a. It can be observed that the intensity of the internal charge transfer complex (ICT) gradually increases, and the ICT absorption maximum shifts from 692 nm for the 0% glycol polymer (P-0) to 718 nm for the 100% glycol polymer (P-100). Photothermal deflection spectroscopy (PDS) in solid state was carried out (Figure S20) where a growing deep tail state was observed when

DOI: 10.1021/acs.chemmater.8b00321
Chem. Mater. 2018, 30, 2945−2953

the glycol percentage was increased. The thin-film PL spectra of the polymer series are presented in Figure 2b where a decrease in the PL can be observed as well as a red-shift of approximately 75 nm as the glycol side chain fraction increases. The integrated photoluminescence intensity decreases by a factor of 4 as the glycol side chain fraction increases from 0 to 100% (Figure S21), though we note that this may be exaggerated, as the entire spectrum cannot be captured by the silicon CCD employed here.

Molecular weight analysis was carried out by gel permeation chromatography (GPC) in chlorobenzene, and the results are summarized in Table 1. It was observed that copolymers with

Table 1. Properties of the Polymer Series

polymer	glycol %	M_n[a] (kDa)	M_w[a] (kDa)	optical band gap (eV)[b]	IP[c] (eV)	EA[d]
P-0	0	18	33	1.42	5.71	4.29
P-10	10	18.4	32.8	1.41	5.71	4.30
P-25	25	15.3	27.1	1.39	5.66	4.27
P-50	50	19.0	31.0	1.38	5.63	4.25
P-75	75	16.7*	22.8*	1.35	5.55	4.20
P-90	90	7.8*	12.4*	1.34	5.57	4.23
P-100	100	7.2*	9.0*	1.33	5.50	4.17

[a]GPC measurements were carried out in chlorobenzene, * observation of bimodular elution of the copolymer (Figures S17 and S18). [b]The optical band gap was extracted from the onset of the absorption spectra (Figure 2a). [c]IP was measured by PESA. [d]EA was calculated by subtracting the optical band gap from the IP values obtained from PESA (this calculation neglects the electron binding energy).

glycol chain densities > P-50 formed aggregates in chlorobenzene (Figure S16b), resulting in the formation of bimodal fractions as presented in Figures S17 and S18. To avoid overestimating the molecular weight distribution, the signal observed for short elution times (high molecular weights) was neglected, and additional mass spectrometry (MALDI-ToF) was carried out to analyze the chain length of the copolymers. Copolymers containing glycol side chains were detected with chain lengths >15 kDa (Figure S19). The alkyl chain polymer could not be detected by mass spectrometry, most likely due to the absence of polar side chains, which is assumed to enhance the ionization of molecules during the mass spectrometry measurement. The ^{1}H NMR spectra of the copolymers are shown in Figure S15. The methylene group adjacent to the NDI core gives a characteristic signal for alkyl or glycol side chains, with chemical shifts at 4.5 ppm for glycol and 4.2 ppm for alkyl side chain, respectively. It is therefore possible to distinguish between the side chains and calculate the ratio of alkyl to glycol side chains of the random copolymers.

The thermal stability of the polymers decreased from 427 °C for the P-0 to 340 °C for P-90 (Figure S23). Differential scanning calorimetry (DSC) was carried out to measure the melting and crystallization temperatures of the polymers. P-0 shows well pronounced melting and recrystallization temperatures at 303 and at 285 °C, respectively (Figure S24), in agreement with the literature.[37,38] The substitution of 10% alkyl with glycol chains increases the melting and crystallization temperatures to 305 and 293 °C, respectively (P-10), while larger percentages of glycol chain densities suppress both the melting and crystallization temperatures.

Ionization potentials (IP) of the polymer series were measured by photoelectron spectroscopy in air (PESA), and the results are summarized in Table 1. The incorporation of glycol chain slightly decreases the IP from 5.7 (P-0) to 5.5 eV (P-100). A similar trend has been observed for copolymers based on polythiophenes where the glycol analogue exhibited a lower IP compared to the alkyl chain analogue.[6,39] These findings suggest that the glycol side chain might interact with the polymer backbone and therefore increase the electron density of the copolymers, a plausible reason for the observed decrease of the IP.

Following polymer synthesis and characterization, OECTs were fabricated to study the influence of the side chain on the performance of the copolymers where the figure of merit of an individual OECT is the transconductance (g_m). To allow for a fair comparison of the device performance, all transistors were fabricated using the same footprint.[20,40] The transconductance was normalized by the thickness of the active layer, and the results are presented in Table 2. The copolymers P-90 and P-100 show the highest performance (~0.2 S/cm) within the series, while the addition of more than 10% alkyl side chains decreased g_m, resulting in a drop for P-75 (0.14 S/cm) and P-50 (0.06 S/cm). In addition, an increase of the injection barrier of electrons can be observed as well as hysteresis for forward and backward biasing (see output and transfer curves in Figure S27). P-25 and P-10 showed signs of turn on at gate biases >0.6 V but suffered from low currents and hysteretic operation. P-0 could not be operated as an electrochemical transistor at the biases and dimensions probed here; increased biasing is limited by operation in water due to electrolysis of water or reduction of oxygen.[41] An increase of g_m is expected to be observed when the thickness of the active layer was increased, as this is characteristic of OECTs.[20] For example, a film of P-90 prepared by drop casting, which is approximately 20 times thicker than the spin-cast device reported here, achieved a transconductance of >40 μS (Figure S28). The expected 20-fold increase was exceeded by a factor of 2, which could be the result of irregular film thickness across the device upon drop casting.

To understand the differences in performance of the polymers in OECTs, we investigated the influence of the side chain substitution on (i) the interaction with aqueous electrolytes, (ii) the electrochemical properties (cyclic voltammetry (CV) and electrochemical impedance spectroscopy (EIS) measurements), (iii) the charge carrier mobility, and (iv) the change in morphology.

The interactions between copolymers and aqueous electrolytes were studied by contact angle measurements as well as quartz crystal microbalance with dissipation monitoring (QCM-D). The results are shown in Figure 3a, where it can be observed that the contact angle with DI water gradually decreases from 102° (P-0) to 58° (P-100), showing that the polarity of the copolymers increases significantly. The swelling experiments performed in 0.1 M NaCl aqueous solution showed significant differences in the hydration behavior. Copolymers from P-0 to P-50 showed a low degree of swelling (<10%) which increased dramatically for P-75 (12%), P-90 (42%) and P-100 (102%). This demonstrates that the addition of alkyl side chains has a significant influence on the swelling in aqueous electrolytes, which can influence the properties of the copolymers when they are in contact with an aqueous electrolyte or even under ambient conditions. It is interesting to note that the heptakis(ethylene glycol) chains on the NDI repeat unit increase the swelling significantly, while only 10% swelling was observed for a thiophene-based copolymer functionalized with tris(ethylene glycol) side chains. This suggests that extending the length of the glycol side chains has a significant effect on the swelling behavior of the copolymer in aqueous solutions.[6]

CV measurements of copolymer thin films on fluorine doped tin oxide (FTO) coated glass substrates were carried out in 0.1 M NaCl aqueous solution to investigate the effect of the side chain

DOI: 10.1021/acs.chemmater.8b00321
Chem. Mater. 2018, 30, 2945−2953

Table 2. Analysis of the Electrochemical and Electronic Properties of the Copolymers

polymer	reduction onset[a] (V)	C/A (F/cm^2)[b]	thickness (nm)	C^* (F/cm^3)[c]	μ_{el} OFET[e] (cm^2/(V s))	μ_{el} OECT[d] (cm^2/(V s))	normalized g_m (S/cm)[f]
P-0	−1.1	5.46×10^{-5}	35	-	0.132	-	-
P-10	−1.1	5.17×10^{-5}	41	-	0.0514	-	-
P-25	−0.43*	2.10×10^{-4}	39	-	0.00184	-	-
P-50	−0.33	5.46×10^{-4}	31	-	-	-	0.067 (31 nm)
P-75	−0.26	8.62×10^{-4}	39	188.0	-	1.46×10^{-4}	0.141 (39 nm)
P-90	−0.25	8.30×10^{-4}	40	198.2	-	2.38×10^{-4}	0.210 (52 nm)
P-100	−0.24	8.62×10^{-4}	41	192.4	-	1.96×10^{-4}	0.204 (28 nm)

[a]Measurements were carried out in degassed 0.1 M NaCl aqueous solution vs Ag/AgCl, * observation of an additional reduction peak at >1.1 V. [b]The detailed EIS analysis is presented in Figure S26; the electrode area is 3.48×10^{-3} cm^2 with an offset voltage of −0.6 V vs Ag/AgCl. The capacitance values here represent the effective capacitance at 1 Hz. [c]The capacitance values used to extract C^* are from fits of EIS data to a Randle's circuit ($R_s(R_p\|C)$). [d]Electron mobility extracted from OFET (output and transfer curves are presented in the Figure S29). [e]Electron mobility extracted from OECT as previously reported.[40,42] [f]Device dimensions W = 100 μm, L = 10 μm with the indicated thickness; transconductance is normalized by thickness. OECTs were fabricated and characterized as previously reported.[7]

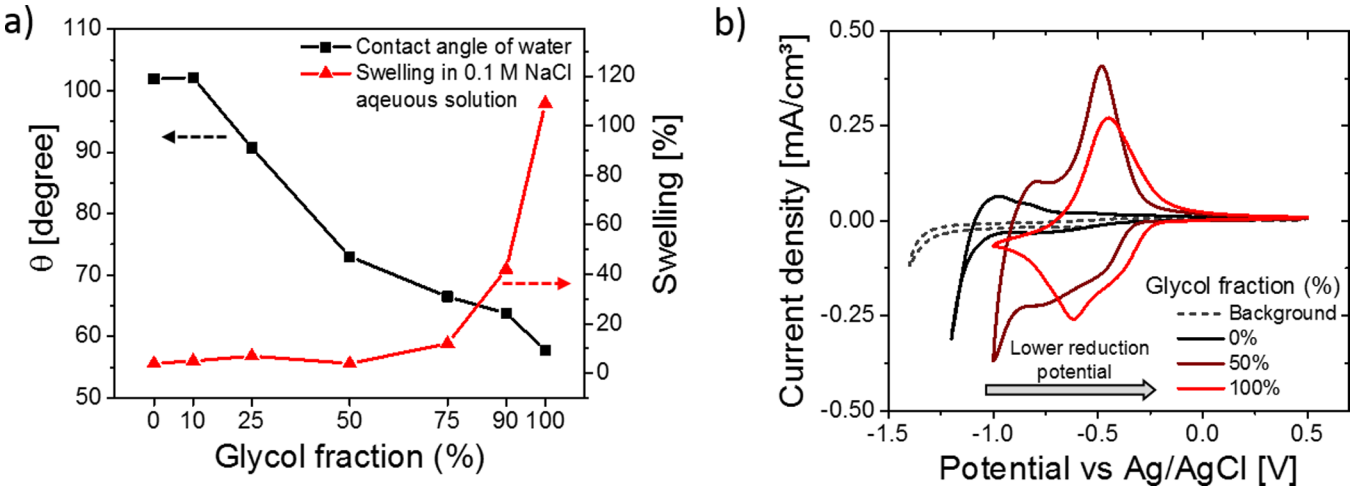

Figure 3. (a) Contact angle and QCM-D measurements of the copolymers in 0.1 M NaCl aqueous solutions and (b) thin film cyclic voltammetry measurements of P-0, P-50, and P-100 and a blank ITO electrode in degassed 0.1 M NaCl aqueous solution with a scan rate of 100 mV/s vs Ag/AgCl.

substitution on the reduction potential. The cyclic voltammograms of three representative copolymers, P-0, P-50, and P-100, are presented in Figure 3b, where it can be observed that the reduction onset shifts from −1.12 V for P-0 to −0.24 V for P-100. As the copolymers have identical backbones, the shift in the reduction potential most likely originates from the difference in ion penetration into the bulk during electrochemical redox reactions. A summary of the CV measurements of all copolymers for five charging and discharging cycles is presented in Table 2 and Figure S25. The copolymers P-0 and P-10 show a reduction peak at voltages higher than −1.0 V. When the glycol percentage is further increased to 25 or 50%, a second peak at lower voltage can be observed which decreases in intensity for P-75 to P-100. When considering the results of the swelling experiments in aqueous solution, one can conclude that the increase in water uptake has a positive effect on the ion penetration into the bulk of the material. For the copolymers which show a higher degree of swelling (P-75 to P-100), a lower reduction potential as well as lower hysteresis during the electrochemical redox reactions can be observed. Copolymers with low glycol percentages (P-0 to P-25) exhibit an increase of the measured currents during repeated charging and discharging of the copolymers, which may imply that the structure can accommodate more sodium ions when repeatedly charged (Figure S25).

The capacitance of the copolymers was investigated by EIS measurements on gold electrodes and 0.1 M NaCl aqueous solution as the supportive electrolyte. The results are summarized in Table 2 and Figure 4a (a detailed summary of the measurements is presented in Figure S26). The copolymers P-75, P-90, and P-100 show comparable capacitance of ∼0.8 mF/cm^2, while lowering the percentages of glycol side chains decreased the capacitance significantly. P-0 and P-10 showed more than an order of magnitude lower capacitance compared to those of P-75, P-90, and P-100. The observed trend in the EIS results is in agreement with the finding that a gradual transition occurs from charge accumulation at or near the semiconductor−electrolyte interface for P-0 and P-10, to volumetric charging where ions are able to penetrate into the bulk of the copolymer for P-75 to P-100. Because volumetric charging is observed for glycol chain densities >75%, a volumetric capacitance C^* can be reported for P-75 (188.0 F/cm^3), P-90 (198.2 F/cm^3), and P-100 (192.4 F/cm^3). This is also valid for thick films where, for example, C^* for P-90 is nearly constant (195 F/cm^3) when the thickness was increased by a factor of 20.

While quantifying the capacity and volumetric charging of the semiconductor film is critical for understanding transistor characteristics such as OECT transconductance, the electronic charge transport (mobility) must also be investigated.[20] Charge carrier mobility of the copolymers was analyzed by both OFET and OECT measurements.[42] The results are presented in Table 2 and Figure 4a where, to extract the electron mobility, each technique was only applicable for the regimes where the polymers perform reasonably well for the specific device types (OFET for P-0 to P-25, OECT for P-75 to P-100). Because both measurements

DOI: 10.1021/acs.chemmater.8b00321
Chem. Mater. 2018, 30, 2945−2953

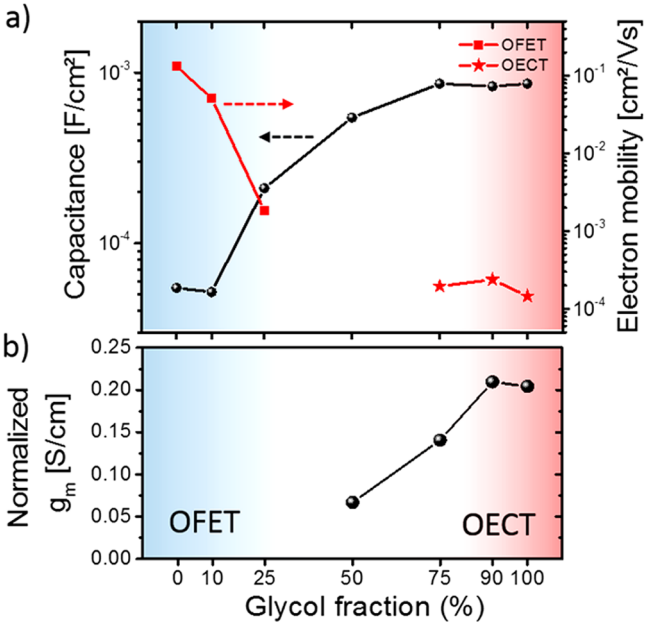

Figure 4. (a) EIS spectroscopy of the polymers at offset voltages of −0.6 V vs Ag/AgCl and electron mobility measurements [OFET (P-0 to P-25) and OECT (P-75 to P-100)] and (b) normalized transconductance of the polymers (OECTs) (devices below 50% could not be operated as OECTs; output and transfer curves of the copolymers are presented in Figure S27).

probe a different type of electron mobility (volumetric charging (OECT) and charge accumulation on the semiconductor/insulator interphase), we wish to emphasize that the results are only used as a qualitative comparison for this broad family of materials. OFET measurements were performed in a glovebox, with additional precautions taken to minimize exposure to water. In addition, the films were not exposed to the ions typical of OECT operation. Under these conditions, the electron mobility from OFET measurements drops by 2 orders of magnitude from P-0 to P-25, reaching values which have been reported for NDI-T2-based copolymers with polar side chains such as glycol-ester (1×10^{-4} cm^2/(V s))[7] or a triethylene glycol side chains (2.2×10^{-4} cm^2/(V s)).[19] Copolymers with glycol percentages >50% demonstrate OECT operation, allowing for measurement of the electron transit time across the channel, which can be used to estimate electron mobility.[40,42] For the extracted mobility values from the OECTs, additional effects need to be considered compared to the OFET measurements. These include the swelling of the polymers in water and the interaction of the reduced polymer with the cations, which are assumed to influence the electron mobility of the copolymers. The effects of the solvent and ions were not thoroughly investigated with respect to electron mobility in this work. The overall decrease of the electron mobility in OECTs is in agreement with recent work on polycationic electrolyte gated FETs with P(NDI2OD-T2), showing a decrease in the electron mobility (10^{-3}–10^{-2} cm^2/(V s))[43−45] compared to mobility measurements of the same polymer in OFETs (0.06–0.85 cm^2/(V s)).[36,38] The strong swelling of the NDI-T2 copolymers with a large fraction of glycol chains could also increase water-induced trapping.[46] Recently, Kiefer et al. observed a drop of the conductance of a n-type doped NDI-T2 copolymers with polar glycol side by a factor of 5 when the device was brought in contact with water, indicating that solvent molecules from the electrolyte might affect the electron transport significantly.[18]

Given the OFET device operation for the low glycol percentage copolymers in dry, ion-free conditions, the energetic contributions and morphological/microstructural changes due to the side chains are believed to be the primary contributors to deficiencies in electron mobility. The morphology of the copolymers was analyzed by GIWAXS measurements on silicon substrates, and the results are summarized in Figure S33. The texture of the copolymers is reminiscent of classic P(NDI2OD-T2), predominantly face-on with clear mixed polymorphs (Form I and II).[47,48] As reported by Brinkmann et al.,[48] the polymorph Form I shows a stronger overlap of the NDI repeat units, while Form II shows a strong overlap of the NDI and T2 repeat units when considering the π-stacking of the backbones. Over the P-0 to P-100 series, there is a general increase of the lamellar spacing (from in plane scattering) as well as a concerted decrease in the (010) π–π stacking distance with incremental incorporation of glycol side chains (Figure S32). The backbone associated scattering with both Form II (noted as (001)) and Form I (noted as (001)′) polymorphs appears across all samples, with relatively unchanged spacings. The ratio of the (001)′ to (001) peak areas provides a relative comparison of the content of Form I vs Form II crystallites. The addition of linear glycol side chains leads to a decrease in the fraction of mixed stacks (Form II) crystallites from ∼90% to near 60%. This provides further evidence that the incorporation of linear glycol side chains aids in the preference for Form I to aggregate in solution.[48] All films exhibit a large paracrystalline disorder[49,50] ($g \geq 10\%$) (Table S1) in the intermolecular π-stacking direction, with tendency toward higher disorder with higher glycol content. This is accompanied by a qualitative increase in disorder in the lamellar packing supported by broadening (and thus lowering of peak scattered intensity) of higher order peaks. The increase in Urbach disorder energy estimated from PDS measurements ranging from 26.4 meV (P-0) to 40.1 meV (P-100) clearly shows a growing deep tail state upon a higher glycol content (Figure S20). This gradual change in microstructure, including both relative fraction of polymorph and variations in paracrystallinity (of polymers with comparable molecular weight) would noticeably affect the interface mobility as seen in OFETs and charge modulation spectroscopy.[48] The trend toward polymorphism with increasing tendency toward Form I[48] may adversely affect the charge carrier transport. The combination of these findings supports the hypothesis that glycol side chain induced structural changes contribute to disruption in electron mobility.

Additional microwave conductivity photoconductance transient measurements[51] were carried out to get further insight into the charge carrier mobility of the copolymers (Figure S30). In contrast to the OFET and OECT measurements, both the magnitude and lifetime of the photoconductance increases with increasing glycol chain fraction. The increase in photoconductance, expressed as the product of charge carrier yield and microwave-frequency mobility, increases by a factor of ∼5, similar in magnitude to the decrease in photoluminescence quantum yield noted in Figure 2b. The carrier lifetime appears to increase initially and then saturate for high glycol fraction samples. Interpretation of microwave conductivity data is complicated because the product of carrier yield and mobility (the measured quantity) cannot be easily decoupled. Here, we tentatively assign the observed increase in photoconductance to an increase in yield. This is justified by two observations. First, the OFET measurements indicate a significant decrease in the charge carrier mobility as the glycol side chain fraction increases, opposite to the trend observed here. Second, previous studies have indicated that the local

DOI: 10.1021/acs.chemmater.8b00321
Chem. Mater. 2018, 30, 2945−2953

microwave-frequency mobility is remarkably insensitive to the microstructure of conjugated polymers.[52] Thus, it seems most likely that the local mobility has remained roughly constant across this homologous series of polymers, while the yield of charges has increased. This conclusion is consistent with the expected increase in dielectric constant that occurs when alkyl side chains are replaced with glycol chains on a conjugated polymer.[1,53] An increase in dielectric constant would be expected to increase the photoinduced charge yield[54,55] and increase the charge carrier lifetime while simultaneously quenching the photoluminescence: precisely the trends we observe.

To conclude, the observed relationship between transconductance and the percentage of glycol side chain on the NDI-T2 copolymers can be explained by an increased swelling of the copolymers in aqueous electrolytes, enabling the charging of the copolymers at lower potentials. This enhances the uptake up ions and results in an increase of the capacitance of the copolymers by more than one order of magnitude. Analysis of the electron mobility reveals that the drop of the electron mobility for NDI-T2 copolymers with increasing glycol percentage is the reason for the lower transconductance found for the n-type OECTs presented here, compared to state of the art p-type accumulation mode OECTs based on polythiophene copolymers with glycol side chains.[6]

When comparing the normalized g_m (S/cm) of P-100 with p(gNDI-gT2),[7] a previously reported analogue containing an ester group within the glycol side chain as well as replacing the bithiophene (T2) unit to an alkoxybithiophene unit (gT2), it can be observed that the latter has a higher performance in OECTs (1.0 S/cm vs 0.2 S/cm). The reason for a higher performance can be explained when considering the product μC^*,[40] where p(gNDI-gT2) has a 2-fold volumetric capacitance (~400 vs ~200 F/cm^3 at an offset voltage of −0.6 V vs Ag/AgCl) as well as a higher electron mobility (3×10^{-4} vs 2×10^{-4} cm^2/(V s)). Interestingly, the polymer p(gNDI-gT2) with a larger amount of polar side chains has a higher C^* compared to P-100, showing that the choice of the donor−comonomer influences the donor−acceptor interaction of the copolymer, which increases the electron affinity significantly. This further affects the ability of the NDI unit to stabilize more charges on the backbone at lower potentials, which could, if the charge carrier were highly mobile, enhance the performance of n-type OECTs. Recently, it was shown the ladder-type polymers poly(benzimidazobenzophenanthroline) (BBL) can be employed as the active layer in n-type OECTs with slightly higher performance as p(gNDI-gT2),[56] showing that C^* can be increased when side chains are avoided with the drawback of increasing the switching time of the OECT. When the here-presented NDI-T2 copolymers are compared to the NDI-T2 copolymer analogue p(gNDI-T2) with the same backbone motif and above-mentioned glycol-ester side chain,[7] it can be observed that functionalizing the NDI-T2 copolymer with a linear glycol side chains enables the operation of the copolymer to function in a n-type OECT compared to the glycol-ester side chain, although C^* and μ_{el} are comparable of both copolymers (192 F/cm^3, 2×10^{-4} cm^2/(V s) for P-100 compared to 190 F/cm^3, 1×10^{-4} cm^2/(V s) for p(gNDI-T2)). This shows that the choice of the side chain is highly important for the preparation of materials for n-type OECTs. Understanding the effect of the side chains on ion transport is crucial and currently under investigation.

CONCLUSION

In summary, a linear glycol chain was attached to the NDI monomer, and random copolymers with the 2-octyldodecyl analogue were prepared with bithiophene as the comonomer. Copolymers with glycol side chain percentages of 0, 10, 25, 50, 75, 90, and 100 with respect to the alkyl side chain were prepared, and the influence of the glycol side chain percentage on the film capacitance and electron mobility was studied. A strong influence on the optical and electrochemical substitution of the polar side chains was observed when the alkyl chain was gradually exchanged for a glycol side chain. The reduction potential in aqueous solution decreased from −1.1 to −0.2 V when the glycol percentage was increased from 0 to 100%. Additionally, the reversibility of the redox reactions improves with higher glycol chain densities. This has a direct influence on the OECT performance, and only copolymers with glycol percentages >50% could be operated given the limitations on device size and stable operation. This is the first systematic study of how the electron mobility is affected when side chain engineering is used to enable organic semiconductors to function in n-type accumulation mode OECTs. NDI-T2 copolymers with alkyl chains show high electron mobilities, while the electron mobility drops by more than 2 orders of magnitude when more than 25% of the alkyl chains are replaced by polar glycol chains. This shows the importance of chemical design strategies for the development of novel n-type OECT materials.

ASSOCIATED CONTENT

Supporting Information

The Supporting Information is available free of charge on the ACS Publications website at DOI: 10.1021/acs.chemmater.8b00321.

Synthesis and characterizations of the materials: NMR spectroscopy, UV−vis spectroscopy, PL measurements, GPC, mass spectrometry (MALDI), DSC, TGA, PDS, CV, EIS, and GIWAXS measurements (PDF)

AUTHOR INFORMATION

Corresponding Author

*E-mail: (A.G.) ag8013@ic.ac.uk.
*E-mail: (J.R.) jrivnay@northwestern.edu.

ORCID

Alexander Giovannitti: 0000-0003-4778-3615
Piers R.F. Barnes: 0000-0002-7537-8759
Garry Rumbles: 0000-0003-0776-1462
George G. Malliaras: 0000-0002-4582-8501
Iain McCulloch: 0000-0002-6340-7217

Notes

The authors declare no competing financial interest.

ACKNOWLEDGMENTS

We thank Iain Hamilton for assistance in measuring contact angle data and Nathan Cheetham for recording solid state absorption spectra. We acknowledge funding from KAUST and BASF, as well as EPSRC Projects EP/P02484X/1, EP/G037515/1, EP/M005143/1, EP/N509486/1; EC FP7 Project SC2 (610115); and EC H2020 Project SOLEDLIGHT (643791) In addition, this project has received funding from the European Research Council (ERC) under the European Union's Horizon 2020 research and innovation program (grant agreement No 742708). O.G.R. and G.R. acknowledge support for the microwave conductivity and photoluminescence measurements from the Solar Photochemistry Program, Division of Chemical Sciences, Geosciences, and Biosciences, Office of Basic Energy Sciences, U.S. Department of Energy under Contract DE-AC36-08-GO28308 with the National Renewable Energy Laboratory. D.H. gratefully acknowledges support from NSF-GFRP.

DOI: 10.1021/acs.chemmater.8b00321
Chem. Mater. 2018, 30, 2945−2953

REFERENCES

(1) Chen, X.; Zhang, Z.; Ding, Z.; Liu, J.; Wang, L. Diketopyrrolopyrrole-Based Conjugated Polymers Bearing Branched Oligo(Ethylene Glycol) Side Chains for Photovoltaic Devices. *Angew. Chem., Int. Ed.* **2016**, *55*, 10376−10380.

(2) Meng, B.; Song, H.; Chen, X.; Xie, Z.; Liu, J.; Wang, L. Replacing Alkyl with Oligo(ethylene Glycol) as Side Chains of Conjugated Polymers for Close Π−π Stacking. *Macromolecules* **2015**, *48*, 4357−4363.

(3) Kanimozhi, C.; Yaacobi-Gross, N.; Burnett, E. K.; Briseno, A. L.; Anthopoulos, T. D.; Salzner, U.; Patil, S. Use of Side-Chain for Rational Design of N-Type Diketopyrrolopyrrole-Based Conjugated Polymers: What Did We Find Out? *Phys. Chem. Chem. Phys.* **2014**, *16*, 17253−17265.

(4) Kim, R.; Kang, B.; Sin, D. H.; Choi, H. H.; Kwon, S.-K.; Kim, Y.-H.; Cho, K. Oligo(ethylene Glycol)-Incorporated Hybrid Linear Alkyl Side Chains for N-Channel Polymer Semiconductors and Their Effect on the Thin-Film Crystalline Structure. *Chem. Commun.* **2015**, *51*, 1524−1527.

(5) Nielsen, C. B.; Giovannitti, A.; Sbircea, D.-T.; Bandiello, E.; Niazi, M. R.; Hanifi, D. A.; Sessolo, M.; Amassian, A.; Malliaras, G. G.; Rivnay, J.; McCulloch, I. Molecular Design of Semiconducting Polymers for High-Performance Organic Electrochemical Transistors. *J. Am. Chem. Soc.* **2016**, *138*, 10252−10259.

(6) Giovannitti, A.; Sbircea, D.-T.; Inal, S.; Nielsen, C. B.; Bandiello, E.; Hanifi, D. A.; Sessolo, M.; Malliaras, G. G.; McCulloch, I.; Rivnay, J. Controlling the Mode of Operation of Organic Transistors through Side-Chain Engineering. *Proc. Natl. Acad. Sci. U. S. A.* **2016**, *113*, 12017−12022.

(7) Giovannitti, A.; Nielsen, C. B.; Sbircea, D.-T.; Inal, S.; Donahue, M.; Niazi, M. R.; Hanifi, D. A.; Amassian, A.; Malliaras, G. G.; Rivnay, J.; McCulloch, I. N-Type Organic Electrochemical Transistors with Stability in Water. *Nat. Commun.* **2016**, *7*, 13066.

(8) Giovannitti, A.; Thorley, K. J.; Nielsen, C. B.; Li, J.; Donahue, M. J.; Malliaras, G. G.; Rivnay, J.; McCulloch, I. Redox-Stability of Alkoxy-BDT Copolymers and Their Use for Organic Bioelectronic Devices. *Adv. Funct. Mater.* **2018**, 1706325.

(9) Malti, A.; Edberg, J.; Granberg, H.; Khan, Z. U.; Andreasen, J. W.; Liu, X.; Zhao, D.; Zhang, H.; Yao, Y.; Brill, J. W.; Engquist, I.; Fahlman, M.; Wågberg, L.; Crispin, X.; Berggren, M. An Organic Mixed Ion−Electron Conductor for Power Electronics. *Adv. Sci.* **2016**, *3*, 1500305.

(10) Rivnay, J.; Inal, S.; Collins, B. A.; Sessolo, M.; Stavrinidou, E.; Strakosas, X.; Tassone, C.; Delongchamp, D. M.; Malliaras, G. G. Structural Control of Mixed Ionic and Electronic Transport in Conducting Polymers. *Nat. Commun.* **2016**, *7*, 11287.

(11) Yang, L.; Adam, C.; Nichol, G. S.; Cockroft, S. L. How Much Do van Der Waals Dispersion Forces Contribute to Molecular Recognition in Solution? *Nat. Chem.* **2013**, *5*, 1006−1010.

(12) Giridharagopal, R.; Flagg, L. Q.; Harrison, J. S.; Ziffer, M. E.; Onorato, J.; Luscombe, C. K.; Ginger, D. S. Electrochemical Strain Microscopy Probes Morphology-Induced Variations in Ion Uptake and Performance in Organic Electrochemical Transistors. *Nat. Mater.* **2017**, *16*, 737−742.

(13) Zhang, L.; Zeng, H.; Liu, Q. Probing Molecular and Surface Interactions of Comb-Type Polymer Polystyrene-Graft-Poly(ethylene Oxide) (PS-G-PEO) with an SFA. *J. Phys. Chem. C* **2012**, *116*, 17554−17562.

(14) Ratner, M. A.; Shriver, D. F. Ion Transport in Solvent-Free Polymers. *Chem. Rev.* **1988**, *88*, 109−124.

(15) Giovannitti, A.; Nielsen, C. B.; Rivnay, J.; Kirkus, M.; Harkin, D. J.; White, A. J. P.; Sirringhaus, H.; Malliaras, G. G.; McCulloch, I. Sodium and Potassium Ion Selective Conjugated Polymers for Optical Ion Detection in Solution and Solid State. *Adv. Funct. Mater.* **2016**, *26*, 514−523.

(16) Kroon, R.; Kiefer, D.; Stegerer, D.; Yu, L.; Sommer, M.; Müller, C. Polar Side Chains Enhance Processability, Electrical Conductivity, and Thermal Stability of a Molecularly P-Doped Polythiophene. *Adv. Mater.* **2017**, *29*, 1700930.

(17) Liu, J.; Qiu, L.; Portale, G.; Koopmans, M.; ten Brink, G.; Hummelen, J. C.; Koster, L. J. A. N-Type Organic Thermoelectrics: Improved Power Factor by Tailoring Host−Dopant Miscibility. *Adv. Mater.* **2017**, *29*, 1701641.

(18) Kiefer, D.; Giovannitti, A.; Sun, H.; Biskup, T.; Hofmann, A.; Koopmans, M.; Cendra, C.; Weber, S.; Anton Koster, L. J.; Olsson, E.; Rivnay, J.; Fabiano, S.; McCulloch, I.; Müller, C. Enhanced N-Doping Efficiency of a Naphthalenediimide-Based Copolymer through Polar Side Chains for Organic Thermoelectrics. *ACS Energy Lett.* **2018**, *3*, 278−285.

(19) Liu, J.; Qiu, L.; Alessandri, R.; Qiu, X.; Portale, G.; Dong, J.; Talsma, W.; Ye, G.; Sengrian, A. A.; Souza, P. C. T.; Loi, M. A.; Chiechi, R. C.; Marrink, S. J.; Hummelen, J. C.; Koster, L. J. A. Enhancing Molecular n-Type Doping of Donor−Acceptor Copolymers by Tailoring Side Chains. *Adv. Mater.* **2018**, *30*, 1704630.

(20) Rivnay, J.; Leleux, P.; Ferro, M.; Sessolo, M.; Williamson, A.; Koutsouras, D. A.; Khodagholy, D.; Ramuz, M.; Strakosas, X.; Owens, R. M.; Benar, C.; Badier, J.-M.; Bernard, C.; Malliaras, G. G. High-Performance Transistors for Bioelectronics through Tuning of Channel Thickness. *Sci. Adv.* **2015**, *1*, 1−5.

(21) Inal, S.; Rivnay, J.; Leleux, P.; Ferro, M.; Ramuz, M.; Brendel, J. C.; Schmidt, M. M.; Thelakkat, M.; Malliaras, G. G. A High Transconductance Accumulation Mode Electrochemical Transistor. *Adv. Mater.* **2014**, *26*, 7450−7455.

(22) Khodagholy, D.; Rivnay, J.; Sessolo, M.; Gurfinkel, M.; Leleux, P.; Jimison, L. H.; Stavrinidou, E.; Herve, T.; Sanaur, S.; Owens, R. M.; Malliaras, G. G. High Transconductance Organic Electrochemical Transistors. *Nat. Commun.* **2013**, *4*, 2133.

(23) Campana, A.; Cramer, T.; Simon, D. T.; Berggren, M.; Biscarini, F. Electrocardiographic Recording with Conformable Organic Electrochemical Transistor Fabricated on Resorbable Bioscaffold. *Adv. Mater.* **2014**, *26*, 3874−3878.

(24) Zeglio, E.; Vagin, M.; Musumeci, C.; Ajjan, F. N.; Gabrielsson, R.; Trinh, X. T.; Son, N. T.; Maziz, A.; Solin, N.; Inganäs, O. Conjugated Polyelectrolyte Blends for Electrochromic and Electrochemical Transistor Devices. *Chem. Mater.* **2015**, *27*, 6385−6393.

(25) de Leeuw, D. M.; Simenon, M. M. J.; Brown, A. R.; Einerhand, R. E. F. Stability of N-Type Doped Conducting Polymers and Consequences for Polymeric Microelectronic Devices. *Synth. Met.* **1997**, *87*, 53−59.

(26) Strakosas, X.; Bongo, M.; Owens, R. M. The Organic Electrochemical Transistor for Biological Applications. *J. Appl. Polym. Sci.* **2015**, *132*, 41735.

(27) Rivnay, J.; Inal, S.; Salleo, A.; Owens, R. M.; Berggren, M.; Malliaras, G. G. Organic Electrochemical Transistors. *Nat. Rev. Mater.* **2018**, *3*, 17086.

(28) Khodagholy, D.; Doublet, T.; Quilichini, P.; Gurfinkel, M.; Leleux, P.; Ghestem, A.; Ismailova, E.; Hervé, T.; Sanaur, S.; Bernard, C.; Malliaras, G. G. In Vivo Recordings of Brain Activity Using Organic Transistors. *Nat. Commun.* **2013**, *4*, 1575.

(29) Higgins, S. G.; Muir, B. V. O.; Dell'Erba, G.; Perinot, A.; Caironi, M.; Campbell, A. J. Complementary Organic Logic Gates on Plastic Formed by Self-Aligned Transistors with Gravure and Inkjet Printed Dielectric and Semiconductors. *Adv. Electron. Mater.* **2016**, *2*, 1500272.

(30) Hütter, P. C.; Rothländer, T.; Scheipl, G.; Stadlober, B. All Screen-Printed Logic Gates Based on Organic Electrochemical Transistors. *IEEE Trans. Electron Devices* **2015**, *62*, 4231−4236.

(31) Chen, Z.; Zheng, Y.; Yan, H.; Facchetti, A. Naphthalenedicarboximide- vs Perylenedicarboximide-Based Copolymers. Synthesis and Semiconducting Properties in Bottom-Gate N-Channel Organic Transistors. *J. Am. Chem. Soc.* **2009**, *131*, 8−9.

(32) Sessolo, M.; Khodagholy, D.; Rivnay, J.; Maddalena, F.; Gleyzes, M.; Steidl, E.; Buisson, B.; Malliaras, G. G. Easy-to-Fabricate Conducting Polymer Microelectrode Arrays. *Adv. Mater.* **2013**, *25*, 2135−2139.

(33) Mahou, R.; Wandrey, C. Versatile Route to Synthesize Heterobifunctional Poly(ethylene Glycol) of Variable Functionality for Subsequent Pegylation. *Polymers (Basel, Switz.)* **2012**, *4*, 561−589.

(34) Svedhem, S.; Hollander, C.-Å.; Shi, J.; Konradsson, P.; Liedberg, B.; Svensson, S. C. T. Synthesis of a Series of Oligo(ethylene Glycol)-

DOI: 10.1021/acs.chemmater.8b00321
Chem. Mater. 2018, 30, 2945−2953

Terminated Alkanethiol Amides Designed to Address Structure and Stability of Biosensing Interfaces. *J. Org. Chem.* **2001**, *66*, 4494−4503.
(35) Higginbotham, H. F.; Maniam, S.; Langford, S. J.; Bell, T. D. M. New Brightly Coloured, Water Soluble, Core-Substituted Naphthalene Diimides for Biophysical Applications. *Dyes Pigm.* **2015**, *112*, 290−297.
(36) Chen, Z.; Zheng, Y.; Yan, H.; Facchetti, A. Naphthalenedicarboximide- vs Perylenedicarboximide-Based Copolymers. Synthesis and Semiconducting Properties in Bottom-Gate N-Channel Organic Transistors. *J. Am. Chem. Soc.* **2009**, *131*, 8−9.
(37) Madorsicy, S. L.; Straus, S. Thermal Degradation of Polyethylene Oxide and Polypropylene Oxide. *J. Polym. Sci.* **1959**, *36*, 183−194.
(38) Yan, H.; Chen, Z.; Zheng, Y.; Newman, C.; Quinn, J. R.; Dötz, F.; Kastler, M.; Facchetti, A. A High-Mobility Electron-Transporting Polymer for Printed Transistors. *Nature* **2009**, *457*, 679−686.
(39) Chen, X.; Zhang, Z.; Liu, J.; Wang, L. A Polymer Electron Donor Based on Isoindigo Units Bearing Branched Oligo(ethylene Glycol) Side Chains for Polymer Solar Cells. *Polym. Chem.* **2017**, *8*, 5496−5503.
(40) Inal, S.; Malliaras, G. G.; Rivnay, J. Benchmarking Organic Mixed Conductors for Transistors. *Nat. Commun.* **2017**, *8*, 1767.
(41) de Leeuw, D. M.; Simenon, M. M. J.; Brown, a. R.; Einerhand, R. E. F. Stability of N-Type Doped Conducting Polymers and Consequences for Polymeric Microelectronic Devices. *Synth. Met.* **1997**, *87*, 53−59.
(42) Rivnay, J.; Ramuz, M.; Leleux, P.; Hama, A.; Huerta, M.; Owens, R. M. Organic Electrochemical Transistors for Cell-Based Impedance Sensing. *Appl. Phys. Lett.* **2015**, *106*, 43301.
(43) Nketia-Yawson, B.; Tabi, G. D.; Noh, Y.-Y. Low-Voltage Operated Solid-State Electrolyte-Gated Ambipolar Organic Field-Effect Transistors. *Org. Electron.* **2018**, *52*, 257−263.
(44) Choi, J.-H.; Xie, W.; Gu, Y.; Frisbie, C. D.; Lodge, T. P. Single Ion Conducting, Polymerized Ionic Liquid Triblock Copolymer Films: High Capacitance Electrolyte Gates for N-Type Transistors. *ACS Appl. Mater. Interfaces* **2015**, *7*, 7294−7302.
(45) Malti, A.; Gabrielsson, E. O.; Berggren, M.; Crispin, X. Ultra-Low Voltage Air-Stable Polyelectrolyte Gated N-Type Organic Thin Film Transistors. *Appl. Phys. Lett.* **2011**, *99*, 63305.
(46) Di Pietro, R.; Fazzi, D.; Kehoe, T. B.; Sirringhaus, H. Spectroscopic Investigation of Oxygen- and Water-Induced Electron Trapping and Charge Transport Instabilities in N-Type Polymer Semiconductors. *J. Am. Chem. Soc.* **2012**, *134*, 14877−14889.
(47) Rivnay, J.; Toney, M. F.; Zheng, Y.; Kauvar, I. V.; Chen, Z.; Wagner, V.; Facchetti, A.; Salleo, A. Unconventional Face-On Texture and Exceptional In-Plane Order of a High Mobility N-Type Polymer. *Adv. Mater.* **2010**, *22*, 4359−4363.
(48) Brinkmann, M.; Gonthier, E.; Bogen, S.; Tremel, K.; Ludwigs, S.; Hufnagel, M.; Sommer, M. Segregated versus Mixed Interchain Stacking in Highly Oriented Films of Naphthalene Diimide Bithiophene Copolymers. *ACS Nano* **2012**, *6*, 10319−10326.
(49) Rivnay, J.; Noriega, R.; Kline, R. J.; Salleo, A.; Toney, M. F. Quantitative Analysis of Lattice Disorder and Crystallite Size in Organic Semiconductor Thin Films. *Phys. Rev. B: Condens. Matter Mater. Phys.* **2011**, *84*, 45203.
(50) Noriega, R.; Rivnay, J.; Vandewal, K.; Koch, F. P. V; Stingelin, N.; Smith, P.; Toney, M. F.; Salleo, A. A General Relationship between Disorder, Aggregation and Charge Transport in Conjugated Polymers. *Nat. Mater.* **2013**, *12*, 1038−1044.
(51) Reid, O. G.; Moore, D. T.; Li, Z.; Zhao, D.; Yan, Y.; Zhu, K.; Rumbles, G. Quantitative Analysis of Time-Resolved Microwave Conductivity Data. *J. Phys. D: Appl. Phys.* **2017**, *50*, 493002.
(52) O'Connor, B. T.; Reid, O. G.; Zhang, X.; Kline, R. J.; Richter, L. J.; Gundlach, D. J.; DeLongchamp, D. M.; Toney, M. F.; Kopidakis, N.; Rumbles, G. Morphological Origin of Charge Transport Anisotropy in Aligned Polythiophene Thin Films. *Adv. Funct. Mater.* **2014**, *24*, 3422−3431.
(53) Torabi, S.; Jahani, F.; Van Severen, I.; Kanimozhi, C.; Patil, S.; Havenith, R. W. A.; Chiechi, R. C.; Lutsen, L.; Vanderzande, D. J. M.; Cleij, T. J.; Hummelen, J. C.; Koster, L. J. A. Strategy for Enhancing the Dielectric Constant of Organic Semiconductors Without Sacrificing Charge Carrier Mobility and Solubility. *Adv. Funct. Mater.* **2015**, *25*, 150−157.
(54) Onsager, L. Initial Recombination of Ions. *Phys. Rev.* **1938**, *54*, 554−557.
(55) Braun, C. L. Electric Field Assisted Dissociation of Charge Transfer States as a Mechanism of Photocarrier Production. *J. Chem. Phys.* **1984**, *80*, 4157−4161.
(56) Sun, H.; Vagin, M.; Wang, S.; Crispin, X.; Forchheimer, R.; Berggren, M.; Fabiano, S. Complementary Logic Circuits Based on High-Performance N-Type Organic Electrochemical Transistors. *Adv. Mater.* **2018**, *30*, 1704916.

DOI: 10.1021/acs.chemmater.8b00321
Chem. Mater. 2018, 30, 2945−2953